2,2′-Azobis(pyridine) (abpy) as a Multiply Reducible Tetradentate Ligand. EPR Evidence for the Configurational Dependence of Intramolecular Electron Transfer in the Stereoisomeric Tris-Chelate Complexes $[Ru(abpy)_n(bpy)_{3-n}]^m$ (n = 2, 3; m = 2+ to 3-)

Michael Krejčík,[1a] Stanislav Záliš,[1a] Jiří Klíma,[1a] David Sýkora,[1b] Walter Matheis,[1c] Axel Klein,[1c] and Wolfgang Kaim*,[1c]

J. Heyrovsky Institute of Physical Chemistry and Electrochemistry, Czech Academy of Sciences, Dolejškova 3, CS-18223 Prague, Czech Republic, Tessek Ltd., Križovnicka 16, CS-11000 Prague, Czech Republic, and Institut für Anorganische Chemie, Universität Stuttgart, Pfaffenwaldring 55, D-7000 Stuttgart 80, Germany

Received February 10, 1993

The mononuclear title complexes can exist as stereoisomers due to the unsymmetrically chelating α-azimino functionality of the abpy ligand. Both *fac* and *mer* isomers of $[Ru(abpy)_3]^{2+}$ and two out of the three possible diastereoisomers of $[Ru(abpy)_2(bpy)]^{2+}$ were isolated via HPLC and identified by virtue of their ^1H NMR spectra. Electrochemical potentials for several one-electron reduction steps and UV/vis spectroelectrochemical features vary to a small but detectable degree for the respective pairs of isomers. The absence of a room-temperature EPR signal for one of the two isolated isomers of $[Ru^{II}(abpy^-)(abpy)(bpy)]^{\bullet+}$ demonstrates the structural requirements for intramolecular electron transfer. A $^{99,101}Ru$ EPR hyperfine coupling of about 0.8 mT was established for the previously reported radical ion $[Ru(abpy)(bpy)_2]^{\bullet+}$. The free α-azimino chelate sites in mononuclear complexes of abpy render these systems suitable for the construction of polynuclear compounds. The exceptional π-acceptor capability of abpy is illustrated by the reversible acceptance of at least eight electrons by the dinuclear complex $\{[Ru(bpy)_2]_2(\mu,\eta^4\text{-abpy})\}^n$.

Introduction

The stereochemical aspects of ruthenium "polypyridine" chemistry[2] are being increasingly recognized and appreciated in connection with supramolecular chemistry, including stereocontrolled energy and electron transfer[3,4] and molecular recognition by biopolymers.[5] In this work we describe the isolation via chromatography and the spectroscopic and electrochemical characterization of positional isomers arising from the combinations $[Ru(abpy)_n(bpy)_{3-n}]^m$ (abpy = 2,2′-azobis(pyridine); bpy = 2,2′-bipyridine; n = 2, 3; m = 2+ to 3-). Whereas the positional isomers of related complexes with the monochelating 2-(phenylazo)pyridine (pap) instead of abpy were described previously,[6] the bischelating and very strongly π-accepting 2,2′-azobis(pyridine)[7] was not yet studied in this respect. Bis-chelate ligands[7,8] such as abpy (**1**) are of current interest because they are capable of connecting metal centers in the stepwise construction of polynuclear arrangements.[9] The study of multiple reduction of positional isomers by cyclic voltammetry and EPR spectroscopy should also reveal low-activation pathways for intramolecular electron transfer between metal-coordinated ligands;[10] reduced polypyridines have proven to exhibit rather large such barriers due to the tris-chelate arrangement of radical ligands.[10a]

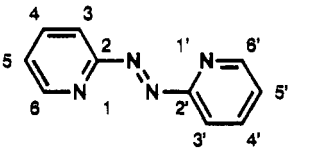

abpy
s-cis/(NN)-trans/s-cis conformation
1

(1) (a) Czech Academy of Sciences. (b) Tessek Ltd. (c) Universität Stuttgart.
(2) (a) Krause, R. A. *Struct. Bonding (Berlin)* **1987**, *67*, 1. (b) Juris, A.; Balzani, V.; Barigellettti, F.; Campagna, S.; Belser, P.; von Zelewsky, A. *Coord. Chem. Rev.* **1988**, *84*, 85.
(3) (a) Lehn, J.-M. *Angew. Chem.* **1988**, *100*, 91; *Angew. Chem., Int. Ed. Engl.* **1988**, *27*, 89. (b) Lehn, J.-M. *Angew. Chem.* **1990**, *102*, 1347; *Angew. Chem., Int. Ed. Engl.* **1990**, *29*, 1304.
(4) Balzani, V. *Tetrahedron* **1992**, *48*, 10443.
(5) Jenkins, Y.; Barton, J. K. *J. Am. Chem. Soc.* **1992**, *114*, 8736 and literature cited therein.
(6) (a) Krause, R. A.; Krause, K. *Inorg. Chem.* **1982**, *21*, 1714. (b) Bao, T.; Krause, K.; Krause, R. A. *Inorg. Chem.* **1988**, *27*, 759. (c) Deb, A. K.; Kakoti, M.; Goswami, S. *J. Chem. Soc., Dalton Trans.* **1991**, 3249. (d) Ghosh, P.; Pramanik, A.; Bag, N.; Chakravorty, A. *J. Chem. Soc., Dalton Trans.* **1992**, 1883. (e) Kakoti, M.; Deb, A. K.; Goswami, S. *Inorg. Chem.* **1992**, *31*, 1302. (f) Choudhury, S.; Kakoti, M.; Deb, A. K.; Goswami, S. *Polyhedron* **1992**, *11*, 3183.
(7) (a) Baldwin, A.; Lever, A. B. P.; Parish, R. V. *Inorg. Chem.* **1969**, *8*, 107. (b) Kohlmann, S.; Ernst, S.; Kaim, W. *Angew. Chem.* **1985**, *97*, 698; *Angew. Chem., Int. Ed. Engl.* **1985**, *24*, 684. (c) Kaim, W.; Kohlmann, S. *Inorg. Chem.* **1987**, *26*, 68. Kaim, W.; Kohlmann, S. *Inorg. Chem.* **1987**, *26*, 1469. (e) Ernst, S.; Kasack, V.; Kaim, W. *Inorg. Chem.* **1988**, *27*, 1146. (f) Nevin, W. A.; Lever, A. B. P. *Anal. Chem.* **1988**, *60*, 727. (g) Ernst, S. D.; Kaim, W. *Inorg. Chem.* **1989**, *28*, 1520. (h) Kaim, W.; Ernst, S.; Kasack, V. *J. Am. Chem. Soc.* **1990**, *112*, 173. (i) Kaim, W.; Kohlmann, S. *Inorg. Chem.* **1990**, *29*, 2909. (j) Kaim, W.; Kohlmann, S. *Inorg. Chem.* **1986**, *25*, 3442.
(8) Kaim, W.; Kohlmann, S.; Jordanov, J.; Fenske, D. *Z. Anorg. Allg. Chem.* **1991**, *598/599*, 217.
(9) (a) Denti, G.; Campagna, S.; Sabatino, L.; Serroni, S.; Ciano, M.; Balzani, V. *Inorg. Chem.* **1990**, *29*, 4750. (b) Denti, G.; Campagna, S.; Serroni, S.; Ciano, M.; Balzani, V. *J. Am. Chem. Soc.* **1992**, *114*, 2944. (c) Serroni, S.; Denti, G. *Inorg. Chem.* **1992**, *31*, 4251 and references cited. (d) Serroni, S.; Denti, G.; Campagna, S.; Juris, A.; Ciano, M.; Balzani, V. *Angew. Chem.* **1992**, *104*, 1540; *Angew. Chem., Int. Ed. Engl.* **1992**, *31*, 1493.
(10) (a) Morris, D. E.; Hanck, K. W.; DeArmond, M. K. *J. Am. Chem. Soc.* **1983**, *105*, 3032. (b) DeArmond, M. K.; Hanck, K. W.; Wertz, D. W. *Coord. Chem. Rev.* **1985**, *64*, 65. (c) Ohsawa, Y.; DeArmond, M. K.; Hanck, K. W.; Moreland, C. G. *J. Am. Chem. Soc.* **1985**, *107*, 5383. (d) Tait, C. T.; MacQueen, D. B.; Donohoe, R. J.; DeArmond, M. K.; Hanck, K. W.; Wertz, D. W. *J. Phys. Chem.* **1986**, *90*, 1766. (e) Gex, J. N.; DeArmond, M. K.; Hanck, K. W. *J. Phys. Chem.* **1987**, *91*, 251. (f) Gex, J. N.; Cooper, J. B.; Hanck, K. W.; DeArmond, M. K. *J. Phys. Chem.* **1987**, *91*, 4686. (g) Gex, J. N.; Brewer, W.; Bergmann, K.; Tait, C. D.; DeArmond, M. K.; Hanck, K. W.; Wertz, D. W. *J. Phys. Chem.* **1987**, *91*, 4776.

0020-1669/93/1332-3362$04.00/0

The possible isomerism of the complexes $[Ru(abpy)_n(bpy)_{3-n}]^m$ may be summarized as follows (pairs of enantiomers[11] being *not* considered). For $n = 1$, there is only one positional isomer. For $n = 3$, the alternative is between facial and meridional substitution patterns (**2**). For $n = 2$, there are three positional isomers possible

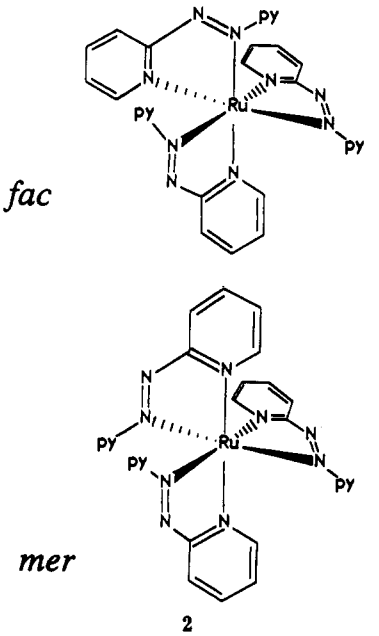

2

(**3**) which, in an adaption of the designation by Krause and Krause,[6a] are referred to as α_1 or α_2 ("ctc" or "cct"),[6f] both with C_2 symmetry, and as β ("ccc"),[6f] with C_1 symmetry.

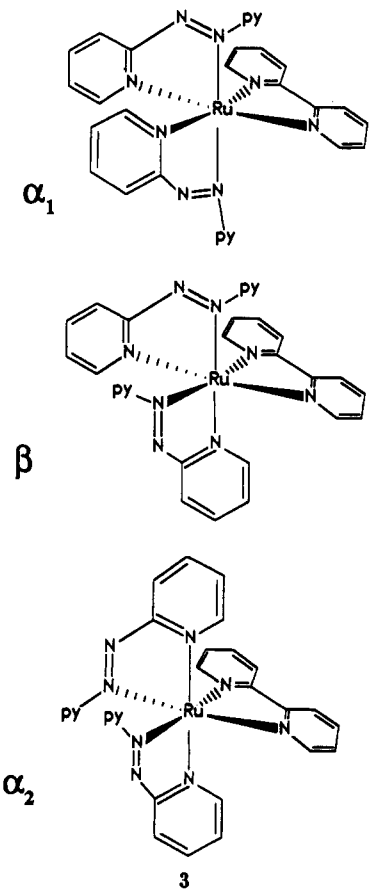

3

The complexes $[Ru(abpy)_n(bpy)_{3-n}]^m$ ($n = 2, 3$) were reduced UV/vis-spectroelectrochemically in up to five reversible one-electron steps. The assignment of the site of electron addition is based on the spectroelectrochemically determined absorptions of the free ligands $bpy^{0/\bullet-/2-}$ and $abpy^{0/\bullet-/2-}$.

The complex $[Ru(abpy)(bpy)_2]^{2+}$, described previously,[7f-h] was reinvestigated in order to assign multiple reduction processes in dry DMF/0.1 M Bu_4NPF_6 and to further analyze the EPR spectrum of the singly reduced species, the cation radical. This EPR spectrum reveals unresolved ligand hyperfine structure of the spin-bearing $abpy^{\bullet-}$ ligand,[10] and it has been possible now to determine the $^{99,101}Ru$ isotope coupling. Finally, the electrochemical reinvestigation of the dinuclear analogue $\{(\mu,\eta^4\text{-abpy})[Ru(bpy)_2]_2\}^{n}$ [7b,e,g] in the negative potential range was undertaken in order to demonstrate the reversible reduction of the coordinated abpy ligand by up to four electrons.

Experimental Section

Materials and Preparations. The ligand abpy[12] and the complexes $Ru(bpy)Cl_4$,[13] $[Ru(abpy)(bpy)_2](PF_6)_2$,[7f,g] $[Ru(abpy)_3](PF_6)_2$ (mixture of *fac* and *mer* isomers),[7g] and $\{(\mu,\eta^4\text{-abpy})[Ru(bpy)_2]_2\}(PF_6)_4$,[7b,e,g] were synthesized according to previously published procedures. The preparation and drying of electrolytes and solvents for electrochemistry were also described recently.[14]

The new compound $[Ru(abpy)_2(bpy)](PF_6)_2$ was obtained as a mixture of isomers via the following typical procedure: An ethanol/water (1/1) solution of 277 mg (1.5 mmol) of abpy and 200 mg (0.5 mmol) of $Ru(bpy)Cl_4$ was heated under reflux for 3 h. After the mixture was cooled to ambient temperature, the complex was precipitated by adding a saturated aqueous solution of ammonium hexafluorophosphate. The isolated and dried complex isomers analyzed correctly (C, H, N) and were subjected to a chromatographic isomer separation.

Chromatographic separations of diastereoisomers from $[Ru(abpy)_3](PF_6)_2$ and $[Ru(abpy)_2(bpy)](PF_6)_2$ were performed using an HPLC system consisting of a Knauer Model 64 pump, a Rheodyne 7125 injection valve, a Knauer UV spectrophotometer, and a TZ 4620 recorder. For preparative separation, a 30 cm × $^3/_4$ in. steel column filled with Tessek Separon SGX (7-μm d_p, Tessek Ltd., Prague) was used with acetone/water/nitric acid (90/5/5) as the mobile phase. For analytical runs, a 15 cm × 3.3 mm Tessek Separon SGX compact glass cartridge (CGC) was employed with acetonitrile/nitric acid/water (90/5/5) as eluent.

Instrumentation, Procedures, and Calculations. The spectroelectrochemical setup, most instruments used for measurements, and the programs (CNDO/S, AM1, EPR computer simulation) were the same as described previously.[14] The AM1-optimized ligand geometries were used in the calculation of the complex $[Ru(abpy)(bpy)_2]^{2+}$, using literature parameters for ruthenium.[15] Open-shell systems were calculated using the restricted Hartree–Fock method within Longuett–Higgins and Pople approximations. All π and the highest lying nonbonding molecular orbitals were included in the configuration interaction. The consistency of the MO basis was preserved throughout neutral and singly and doubly reduced species.

Infrared vibrational spectra were obtained on a Philips PU9800 FTIR spectrometer.[16] ^1H NMR spectra were recorded on a Bruker AM 250 system. Estimated error limits are ±0.01 ppm (^1H NMR chemical shifts), ±2 nm (UV/vis absorption maxima), ±2 cm^{-1} (IR peak positions), and ±0.01 V (redox potentials).

Results

Abpy and bpy. A careful examination of the ^1H NMR spectrum of abpy reveals that this compound exists in two isomeric forms in CD_3CN and $CDCl_3$ solutions (ratio 0.09; Table I). The typical[17] 2-pyridyl signals of the minor species are not due to the hydrogenated form 1,2-bis(2-pyridyl)hydrazine[12] as established

(11) Hua, X.; von Zelewsky, A. *Inorg. Chem.* **1991**, *30*, 3798.

(12) Kirpal, A.; Reiter, L. *Ber. Dtsch. Chem. Ges.* **1927**, *60*, 664.
(13) Krause, R. A. *Inorg. Chem.* **1977**, *22*, 209.
(14) Fees, J.; Kaim, W.; Moscherosch, M.; Matheis, W.; Klíma, J.; Krejčík, M.; Zalíš, S. *Inorg. Chem.* **1993**, *32*, 166.
(15) Tondello, E. *Inorg. Chim. Acta* **1974**, *11*, L5.
(16) Krejčík, M.; Vlček, A. A. *J. Electroanal. Chem. Interfacial Electrochem.* **1991**, *313*, 243.
(17) Cf. Memory, J. D.; Wilson, N. K. *NMR of Aromatic Compounds*; Wiley: New York, 1982.

Table I. ^{1}H NMR Data for 2,2′-Azobis(pyridine) and Complexes[a]

	abpy		$[Ru(abpy)_2(bpy)]^{2+}$		$[Ru(abpy)_3]^{2+}$	
	trans	cis[b]	α_1	β	*fac*	*mer*
$\delta(H^{3,3'})$	7.91	7.37	9.06	9.02	8.92	8.99
	7.98[c]	7.35[c]		8.92		8.92
			8.24	8.67	8.08	8.67
				8.51		*e*
			7.75[d]	7.93[d]		
				e		
$\delta(H^{4,4'})$	8.11	7.92	8.50	8.47	8.46	8.42
	7.93[c]	7.73[c]		8.35		8.33
			8.11	8.11	7.93	*e*
				8.07		
			7.51[d]	*e*		
$\delta(H^{5,5'})$	7.65	7.23	8.05	*e*	7.75	*e*
	7.44[c]	7.02[c]		*e*		*e*
			7.87	7.62	7.41	*e*
				e		7.41
			7.44[d]	7.41[d]		
				7.34[d]		
$\delta(H^{6,6'})$	8.86	8.22	8.51	8.29	7.92	8.27
	8.76[c]	8.09[c]		8.02		8.16
			8.02	*e*	7.51	*e*
				e		
			7.42[d]	7.64[d]		
				7.47[d]		

[a] In CD_3CN, unless stated otherwise. Assignments according to established coupling patterns and spin–spin coupling constants for the 2-pyridyl group:[17] $^3J(H^3–H^4)$ = 8 Hz, $^3J(H^4–H^5)$ = 7 Hz, $^3J(H^5–H^6)$ = 5 Hz. [b] Cis/trans ratio 0.09. [c] In $CDCl_3$. [d] Chemical shifts of protons in 2,2′-bipyridine ligand. [e] Not determined due to overlapping signals.

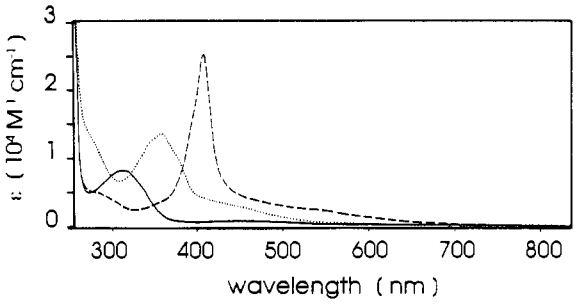

Figure 1. UV/vis absorption spectra of 2,2′-azobis(pyridine) in three oxidation states from spectroelectrochemistry in DMF/0.1 M Bu_4NPF_6: abpy (—); $abpy^{\bullet-}$ (- - -); $abpy^{2-}$ (···).

Table II. UV/Vis Absorption Maxima[a] of Ligands in Three Oxidation States

ligand	abs max ($10^{-4}\epsilon$)
abpy	470 (0.09), 312 (0.87)
$abpy^{\bullet-}$	548 (sh, ≈0.26), 408 (2.65), 360 (sh), 286 (sh)
$abpy^{2-}$	450 (sh), 380 (sh), 358 (1.42), 342 (sh), 275 (sh)
bpy	282 (3.96)
$bpy^{\bullet-}$	582 (1.36), 548 (1.25), 440 (sh), 392 (4.65), 382 (sh), 364 (sh)
bpy^{2-}	550 (sh), 424 (2.60), 396 (sh)

[a] Wavelengths in nm; molar extinction coefficients ϵ in M^{-1} cm^{-1}.

by examination of this compound.[18] The reduction products (1–, 2–) of bpy and abpy (Figure 1) were studied spectroelectrochemically using an OTTLE cell;[16] the absorption maxima are summarized in Table II.

An AM1 calculation of the free ligand 2,2′-azobis(pyridine) gave an almost planar s-cis/(NN)trans/s-cis conformation with the 2-pyridyl rings poised for double chelation as in **1**. This approximately D_{2h}-symmetric conformation was used in calculations of structure parameters and electronic transitions of the three redox states 0, –I, and –II (Table III).

Table III. Calculated Bond Distances[a] and Electronic Transitions[b] of 2,2′-Azobis(pyridine) in Three Oxidation States

	abpy	$abpy^{\bullet-}$	$abpy^{2-}$
		Bond Lengths	
$d(NN')$	1.226	1.278	1.331
$d(NC^2)$	1.455	1.392	1.340
$d(N^1C^2)$	1.366	1.389	1.418
$d(C^2C^3)$	1.422	1.451	1.479
$d(C^3C^4)$	1.395	1.384	1.368
$d(C^4C^5)$	1.393	1.384	1.368
$d(C^5C^6)$	1.408	1.413	1.414
$d(C^6N^1)$	1.341	1.333	1.318
		Transitions	
$n \rightarrow \pi^*$	498 (0.00)		293 (0.006)
$\pi_7 \rightarrow \pi_8$	304 (0.915)	388 (0.885)	
$\pi_8 \rightarrow \pi_9$		556 (0.099)	445 (0.119)
$\pi_8 \rightarrow \pi_{11}$		544 (0.003)	384 (1.472)

[a] Bond distances in Å from AM1 optimization. [b] Transition wavelengths in nm and oscillator strengths (in parentheses) from CNDO/S calculations.

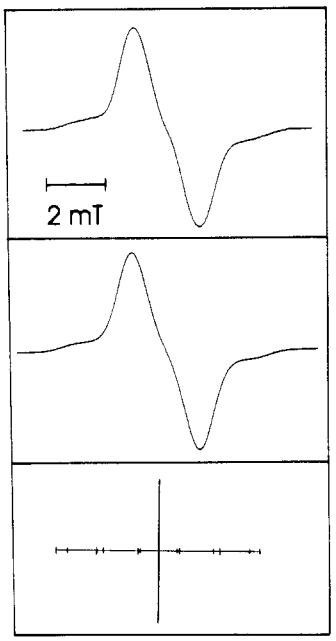

Figure 2. EPR spectrum (top) of spectroelectrochemically generated $[Ru(abpy)(bpy)_2]^+$ in CH_3CN/0.1 M Bu_4NPF_6, computer-synthesized spectrum (center), simulated with the data from Table V and 0.99-mT line width, and stick spectrum (bottom) for the coupling of one unpaired electron with ruthenium (1 Ru) in natural abundance.

$[Ru(abpy)(bpy)_2]^{m+}$. EPR spectroscopy of electrochemically generated $[Ru(abpy)(bpy)_2]^{\bullet+}$ at 295 K in acetonitrile/0.1 M Bu_4NPF_6 reveals a structured main resonance line which is accompanied by satellite features due to ruthenium isotope coupling (Figure 2 (top)): ^{99}Ru has $I = {}^5/_2$, 12.8% natural abundance, and A_{iso} = –37.62 mT; ^{101}Ru has $I = {}^5/_2$, 17.0% natural abundance, and A_{iso} = –42.13 mT.[20] Although the spectral resolution is not sufficient to directly distinguish between the individual isotope features as in the stick spectrum (Figure 2 (bottom)), a computer simulation of the spectrum (Figure 2 (center)) with the coupling constants from Table V gave a good fit. Cyclic voltammetric and UV/vis spectroelectrochemical results are summarized in Tables IV and VI.

(18) ^{1}H NMR of 1,2-bis(2-pyridyl)hydrazine ($CDCl_3$): δ 8.14 ($H^{6,6'}$), 7.49 ($H^{4,4'}$), 6.76 ($H^{3,3'}$), 6.75 ($H^{5,5'}$), 6.51 (H–N).

(19) (a) Bessenbacher, C.; Kaim, W. *Z. Naturforsch.* **1989**, *44B*, 511. (b) Veith, M. *Acta Crystallogr.* **1975**, *B31*, 678.

(20) (a) Kaim, W. *Coord. Chem. Rev.* **1987**, *76*, 187. (b) Anisotropic hyperfine coupling constant A_{iso} from: Symons, M. *Chemical and Biochemical Aspects of Electron-Spin Resonance Spectroscopy*; Van Nostrand Reinhold: New York, 1978; p 176.

Table IV. Electrochemical Data for Ligands and Complexes[a]

abpy
198 K: −1.37(75), −2.12 (ir)
bpy
198 K: −2.55 (75), −3.22 (150)
$[Ru(abpy)_3]^{2+}$, *fac* Isomer
298 K: −0.41 (65), −0.77 (65), −1.32 (65), −1.83 (65), −2.29 (80), −2.77 (110)
198 K: −0.44 (55), −0.76 (55), −1.27 (65), −1.80(120), −2.34 (140), −2.88 (160)
$[Ru(abpy)_3]^{2+}$, *mer* Isomer
298 K: −0.49 (60), −0.84 (60), −1.33 (60), −1.97 (100), −2.39 (100), −2.84 (150)
198 K: −0.50 (50), −0.81 (55), −1.28 (70), −2.00 (190), −2.41 (130), −2.92 (230)
$[Ru(abpy)_2(bpy)]^{2+}$, β Isomer
298 K: −0.54 (60), −0.99 (60), −1.74 (60), −2.08 (60), −2.81 (160)
198 K: −0.59 (50), −1.00 (50), −1.72 (60), −2.08 (100), −2.91 (180)
$[Ru(abpy)_2(bpy)]^{2+}$, α_1 Isomer
298 K: −0.53 (70), −0.92 (70), −1.66 (70), −2.03 (70), −3.00 (100)
198 K: −0.57 (60), −0.91 (55), −1.63 (60), −2.00 (90), −3.02 (110)
$[Ru(abpy)(bpy)_2]^{2+}$
298 K: −0.76 (65), −1.47 (65), −2.11 (65), −2.53 (90)
198 K: −0.81 (60), −1.47 (60), −2.11 (60), −2.52 (60), −3.12 (70)
$[Ru(bpy)_2]_2(abpy)^{4+}$ [b]
298 K: −0.18 (70), −0.81 (70), −1.93 (95),[c] −2.23 (70),[c] −2.35 (70)[c]
198 K: −0.26 (60), −0.87 (60), −1.96 (90),[c] −2.22 (65),[c] −2.31 (65),[c] −2.98 (70)

[a] From cyclic voltammetry at 100 mV/s in DMF/0.1 M Bu_4NPF_6. Potentials in V vs $FeCp_2^{0/+}$; peak potential differences in mV in parentheses. [b] Oxidation potentials in CH_3CN/0.1 M Bu_4NPF_6: +1.26 (85), +1.85 (200). [c] Two-electron processes.

Table V. EPR Data for Cation Radical Complexes[a]

	g		ΔH_{pp}[b]	
	298 K	180 K	298 K	180 K
$[Ru(abpy)(bpy)_2]^{\bullet+}$	1.9983	n.d.	2.1[c]	n.d.
$[Ru(abpy)_2(bpy)]^{\bullet+}$				
α_1 isomer	*d*	1.9858	*d*	2.7
β isomer	1.9978	*e*	2.6[f]	1.4[e]
$[Ru(abpy)_3]^{\bullet+}$				
fac isomer	1.9978	*e*	3.2	1.6[e]
mer isomer	1.9985	*e*	3.5	1.7[e]

[a] From electrochemical reduction of precursor complexes in acetonitrile/0.1 M Bu_4NPF_6. [b] Peak-to-peak distance in mT. [c] Hyperfine structure: $a(^{14}N) = 0.73$ mT (1 N), $a(^{99}Ru) = 0.77$ mT, $a(^{101}Ru) = 0.86$ mT (1 Ru). [d] Not observable at ambient temperature. [e] Axial spectrum with very slight g anisotropy: $g_\parallel < g_\perp$. [f] Structured signal due to unresolved hyperfine splitting.

CNDO/S calculations of the closed-shell system $[Ru(abpy)(bpy)_2]^{2+}$ show that the lowest unoccupied MO (LUMO) is localized at the abpy ligand and that the metal contribution is on the order of about 5%.

$\{(\mu,\eta^4\text{-abpy})[Ru(bpy)_2]_2\}^{m+}$. The dinuclear complex was reinvestigated by cyclic voltammetry in very dry DMF and acetonitrile/0.1 M Bu_4NPF_6. While the previously reported data[7e,g] could essentially be reproduced (Table IV), an extension of the cyclic voltammogram into the negative potential range showed the presence of an additional reversible two-electron reduction step among the two two-electron waves for the reduction of two coordinated bpy pairs. As was noted previously,[7e,g] there is no evidence for a mixture of diastereoisomers; we assume an exclusive formation of the sterically more favored centrosymmetric meso form. The UV/vis-spectroelectrochemical data are listed in Table VI.

$[Ru(abpy)_3]^{m+}$. These homoleptic species can be separated by chromatography into the *fac* and *mer* isomers. Identification was possible by ^1H NMR spectroscopy which, despite the partially incomplete analysis and tentative assignments (Table I), clearly reveals the purity and symmetry of the complexes (Figure 3). Whereas the *fac* isomer exhibits eight signal groups (two 2-pyridyl ABCD systems from three equivalent coordinated and three equivalent "dangling" 2-pyridyl groups), the *mer* isomer shows 24 partially overlapping signals due to six nonequivalent 2-pyridyl ABCD systems.

This assignment is supported by a comparison of IR vibrational spectra, which shows more intense bands at 1466 and especially 1381 cm^{-1} for the more polar *fac* isomer.

Cyclic voltammetry of both isomers of $[Ru(abpy)_3]^{2+}$ yields the expected total of six one-electron reduction steps at very similar but not identical potentials (Table IV). The splitting of the first three steps is unusually large for both isomers, as was noted previously when a mixture of isomers with peaks broadened by unresolved overlap of both isomers was studied.[7g]

When reduced to the monocation radical state at 295 K in acetonitrile, both *fac* and *mer* isomers exhibit unresolved EPR signals (Table V). In both cases, the g anisotropy at 180 K in frozen solution was too small to allow a determination of individual g components. The UV/vis absorption spectra of both nonreduced isomers $[Ru(abpy)_3]^{2+}$ differ slightly (Figure 4); similar differences exist for the spectroelectrochemically studied reduced states (Table VI).

$[Ru(abpy)_2(bpy)]^{m+}$. Two of the three possible isomers (**3**) were obtained as main products after the complete chromatographic separation and purification of complexes $[Ru(abpy)_2(bpy)](PF_6)_2$. ^1H NMR analysis based on the identification of many of the typical resonances (Table I) and on integration allowed us to make a clear distinction: One of the isolated isomers is the unsymmetrical β form, which displays a total of 24 ^1H NMR resonances from six ABCD systems (four from abpy, two from bpy). The other isomer is more symmetrical (α_1 or α_2 with C_2 symmetry) with three 2-pyridyl ABCD systems (Table I). In the IR vibrational spectrum, the most obvious distinction lies in the region between 1300 and 1400 cm^{-1}, where the α isomer exhibits three bands at 1384 (s), 1364 (s), and 1356 cm^{-1} (sh) while β shows only two distinct absorptions at 1379 (m) and 1351 cm^{-1} (vs).

The α and β isomers have rather similar reduction potentials and UV/vis spectra (Tables IV and VI). UV/vis-spectroelectrochemistry also gave comparable results for the reduced forms of the two isomers (Figure 5, Table VI); however, the EPR responses of the singly reduced species $[Ru(abpy)_2(bpy)]^{\bullet+}$ differ considerably: isomer β shows the expected EPR signal at 295 K while isomer α_1 is EPR detectable only at 180 K in frozen solution (Figure 6, Table V).

Discussion

Properties of the abpy Ligand and of Its Complexes with $Ru(bpy)_2^{2+}$. As a typical tetradentate "S frame" ligand,[7c,8] abpy is capable of binding two metals to form edge-shared five-membered chelate rings. The expected[7c] short metal–metal distance was recently confirmed with 4.937 Å for a dicopper(I) complex.[8] Not surprisingly, AM1 geometry optimizations yield the s-cis/(NN)-trans/s-cis conformation (**1**) as the energy minimum; however, NMR studies exhibit the presence of an additional minor species (9%) with generally upfield-shifted resonances (Table I). We attribute these additional signals to the nonplanar and thus not fully conjugated (NN)cis form. This (NN)cis configuration of the free ligand should be less disfavored here than in case of azobenzene because of less steric repulsion between N centers relative to CH;[19a] the center of electron density for a C–H bond has a distance of about 0.95 Å from the sp^2 carbon atom, in contrast to a corresponding value of 0.39 Å for a lone pair at the sp^2 nitrogen.[19]

In addition to the special geometrical features, the unsaturated abpy ligand has a very low-lying π^* MO which is centered mainly

Table VI. UV/Vis Absorption Maxima of Complexes in Different Oxidation States[a]

	IL	MLCT		IL		
			$[Ru(abpy)_3]^n$, *fac* Isomer			
2+		518 (0.99)	474 (sh)	348 (2.56)		
1+		526 (0.96)		344 (2.44)		
0		522 (0.82)		352 (2.85)		
1–	500–700 (sh)			362 (3.97)		
2–	500–700 (sh)			376 (3.48)		324 (sh)
3–	500–700 (sh)			392 (2.92)	368 (2.99)	328 (2.96)
			$[Ru(abpy)_3]^n$, *mer* Isomer			
2+		516 (0.95)	474 (sh)	354 (2.53)		286 (2.00)
1+		544 (1.05)		352 (2.72)		
0		548 (0.82)		360 (3.04)		
1–	500–700 (sh)			362 (3.80)		
2–	500–700 (sh)			370 (3.74)	342 (sh)	
3–	500–700 (sh)			400 (2.82)	350 (3.18)	

	IL or ILCT	MLCT(abpy)	MLCT(bpy)	IL(abpy^n) or IL(bpy^n)	IL(bpy^0)
			$[Ru(abpy)_2(bpy)]^n$, α Isomer		
2+		534 (0.95)	466 (0.62)	332 (2.16)	302 (2.75)
				312 (2.70)	
1+	600 (sh)	540 (0.79)		362 (2.57)	280 (2.97)
0	700 (sh)		460 (sh)	368 (3.50)	290 (3.12)
	560 (sh)				
1–	710 (sh)		490 (sh)	380 (3.97)	292 (3.27)
	590 (sh)				
2–	540 (sh)			380 (3.97)	292 (3.35)
3–	570 (sh)			356 (4.67)	
			$[Ru(abpy)_2(bpy)]^n$, β Isomer		
2+		532 (1.04)	462 (0.57)	342 (2.11)	278 (2.89)
				316 (sh)	
1+	568 (0.82)	510 (sh)		356 (2.45)	286 (3.49)
0	670 (sh)		460 (sh)	356 (3.96)	292 (3.47)
1–	590 (sh)		500 (sh)	372 (4.09)	296 (3.49)
2–	560 (sh)			378 (4.03, br)	296 (3.29)
3–	560 (sh)			350 (4.85)	
			$[Ru(abpy)(bpy)_2]^n$		
2+		512 (0.57)	374 (sh)	320 (sh)	282 (2.93)
1+	604 (0.32)		476 (0.75)	386 (1.55)	294 (3.65)
0	590 (sh)		514 (0.63)	360 (1.73)	294 (3.53)
1–	690 (sh)		514 (0.90)	362 (2.84)	296 (2.16)
	544 (0.89)				
2–	690 (sh)			364 (sh)	
	560 (sh)			344 (3.81)	
			$\{[Ru(bpy)_2]_2(abpy)\}^n$		
4+		756 (0.68)	398 (0.71)		286 (3.43)
		696 (0.50)			
		642 (0.44)			
3+	636 (0.36)		452 (0.65)	374 (0.72)	290 (3.90)
2+			494 (0.83)	346 (1.12)	294 (3.96)
0			506 (0.77)	358 (1.45)	296 (2.96)
2–	590 (sh)		506 (0.87)	360 (1.96)	296 (2.89)
4–	600 (sh)		520 (0.90)	366 (sh)	
				340 (3.00)	

[a] Wavelengths λ_{max} in nm; molar extinction coefficients $10^{-4}\epsilon$ (in parentheses) in M^{-1} cm^{-1}.

(ca. 70%) at the coordinating azo nitrogen atoms[7c,e,j] and which thus favors orbital mixing between abpy and metal centers. Evidence for such orbital mixing comes from the EPR detection of a relatively large[7h] ^{99,101}Ru isotope splitting in $[Ru(abpy)(bpy)_2]^{\bullet+}$ (Figure 2). Whereas the g factor and the apparent hyperfine structure from one (coordinating) azo nitrogen atom leave no doubt that it is the azo function of the abpy ligand which is primarily reduced in the complex, the ratio $a(^{99}Ru)/|A_{iso}(^{99}Ru)| = 0.77\ mT/37.62\ mT = 205 \times 10^{-4}$ is unusually large for radical complexes[20] and thus indicates sizable contributions from the metal to the singly occupied MO.

For assignment of intraligand (IL) bands in spectroelectrochemical studies of the complexes, we have determined the absorption spectra of bpy[21] and abpy (Figure 1) in their singly and doubly reduced states (Table II). CNDO/S calculations (Table III) support the conventional assignment of the weak $n \rightarrow \pi^*$ transition at 470 nm and the $\pi \rightarrow \pi^*$ ($\pi_7 \rightarrow \pi_8$, HOMO $\rightarrow$ LUMO) transition at 312 nm in the neutral form of abpy. The anion radical with the π_8 orbital of the 14-center π system singly occupied exhibits long-wavelength bands at 548 (sh) and 408 nm which are assigned to the transitions $\pi_8 \rightarrow \pi_9$ and $\pi_7 \rightarrow \pi_8$, respectively. The dianion, which may be described as a hydrazido-(2–) ligand, has a shoulder at 450 nm ($\pi_8 \rightarrow \pi_9$) and a band maximum at 358 nm ($\pi_8 \rightarrow \pi_{11}$).

The calculated geometry changes of the abpy$^{0/-/2-}$ series (Table III) confirm that the major changes occur at the azo group (lengthened N–N and shortened C–N bonds) and that the pyridyl rings contribute in terms of a quinonoid resonance structure. Similar effects have been observed experimentally for coordinated pyridylazo ligands in complexes with low-valent metal centers.[22]

The large energy difference between the lowest and the second lowest unoccupied MO in abpy[7c] precludes facile third and fourth

(21) Krejčík, M. Ph.D. Thesis, Charles University, Prague, 1992.

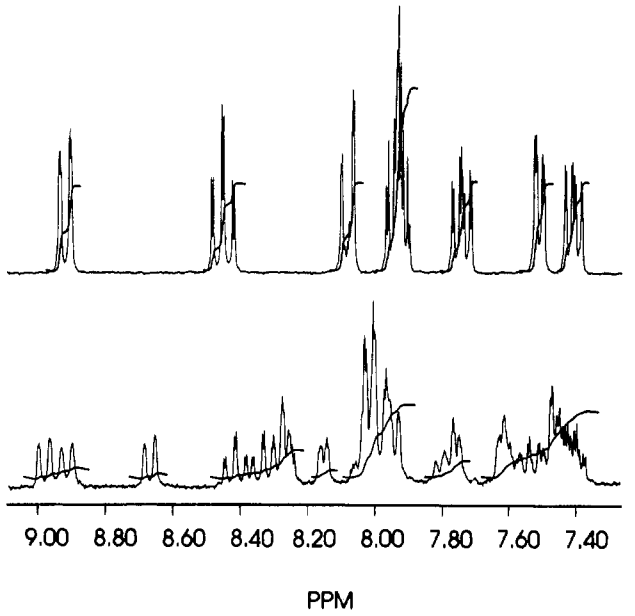

Figure 3. ^{1}H NMR spectra (250 MHz, CD_3CN solutions) of the *fac* (top) and *mer* (bottom) isomers of $[Ru(abpy)_3](PF_6)$ in the pyridyl proton region.

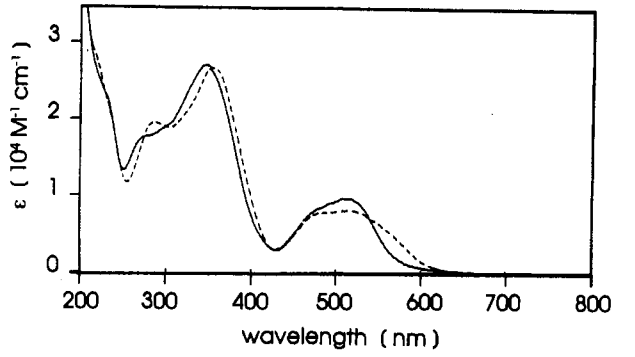

Figure 4. UV/vis absorption spectra of the *fac* (—) and *mer* (- - -) isomers of $[Ru(abpy)_3](PF_6)$ in acetonitrile solution.

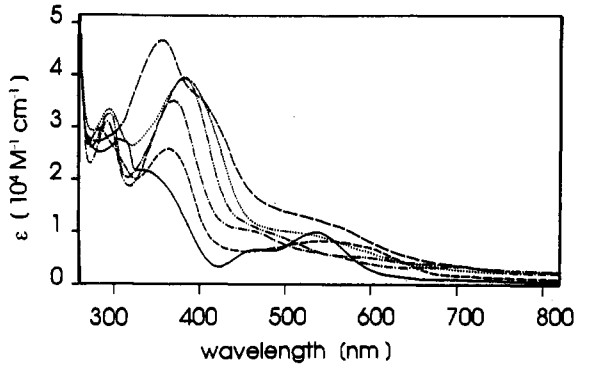

Figure 5. UV/vis absorption spectra from spectroelectrochemistry of the α_1 isomer of $[Ru(abpy)_2(bpy)]^n$ in DMF/0.1 M Bu_4NPF_6: 2+ (—), 1+ (· · ·), 0 (– · –), 1– (– ·· –), 2– (···), 3– (– –).

reductions of the free acceptor molecule; however, the coordination of *two* $Ru(bpy)_2$ dications enabled us now to observe an additional two-electron reduction of η^4-abpy in the complex. The reduction of the complex $\{(\mu,\eta^4\text{-abpy})[Ru(bpy)_2]_2\}(PF_6)_4$ at 198 K proceeds via two abpy-centered one-electron steps and two typically separated[7,8] one-electron reductions of pairs of two coordinated bpy ligands. Between both 2 bpy/2 $bpy^{\bullet-}$ waves is an additional two-electron step which is attributed to two one-electron reduction

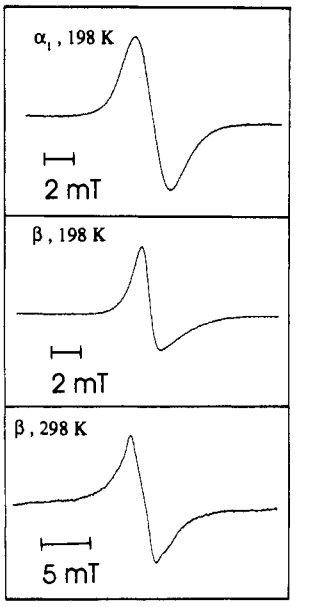

Figure 6. EPR spectra of the α_1 and β isomers of electrochemically generated $[Ru(abpy)_2(bpy)]^+$ at 198 K (top, center) in frozen acetonitrile solution and of the β isomer at 298 K in fluid CH_3CN (bottom). No signal was observed for the α_1 isomer at 298 K.

Scheme I

$$[Ru(abpy)(bpy)_2]^{2+}$$
$$+ e^- \rightleftharpoons - e^-$$
$$[Ru(abpy^{-I})(bpy)_2]^{+}$$
$$+ e^- \rightleftharpoons - e^-$$
$$[Ru(abpy^{-II})(bpy)_2]^{0}$$
$$+ e^- \rightleftharpoons - e^-$$
$$[Ru(abpy^{-II})(bpy^{-I})(bpy)]^{-}$$
$$+ e^- \rightleftharpoons - e^-$$
$$[Ru(abpy^{-II})(bpy^{-I})_2]^{2-}$$
$$+ e^- \rightleftharpoons (- e^-)$$
$$[Ru(abpy^{-II})(bpy^{-II})(bpy^{-I})]^{3-}$$

processes of separated (nonconjugated!) but metal-coordinated 2-pyridyl rings of the py–N⁻–N⁻–py ligand.

The UV/vis-spectroelectrochemical results for $[Ru(abpy)(bpy)_2]^m$ and $\{(\mu,\eta^4\text{-abpy})[Ru(bpy)_2]_2\}^m$ (Table VI) can be interpreted according to Schemes I and II, on the basis of the data for the ligands (Figure 1, Table II).

It is evident from spectroelectrochemistry and from the redox potentials of the free ligands (Tables IV and VI) that the second reduction of abpy occurs at less negative potentials than the first reduction of bpy. Accordingly, the typical absorption band of $abpy^{2-}$ in the complexes at about 360 nm appears instead of the ca. 390 nm band of $abpy^{\bullet-}$ in oxidation states where this assignment may be questioned. Another marker peak is the 290-nm band of nonreduced bpy which is replaced by a ca. 340 nm band in $bpy^{\bullet-}$. After stepwise one-electron reduction of the bridging azo ligand in the dinuclear complex, the weak coupling between separated bpy and 2-pyridyl rings results in three close-lying reversible two-electron steps.

The presence of nonreduced bpy (absorption at 296 nm) in $\{(abpy)[Ru(bpy)_2]_2\}^{2-}$ is evidence for the interpretation of an $abpy^{4-}$ ligand at this stage; however, a characteristic absorption feature for this ligand state could not be established with certainty. The visible parts of the spectra exhibit well-known MLCT bands from transitions to nonreduced abpy or bpy ligands; additional

(22) Lahiri, G. K.; Goswami, S. G.; Falvello, L. R.; Chakravorty, A. *Inorg. Chem.* **1987**, *26*, 3365.

Scheme II

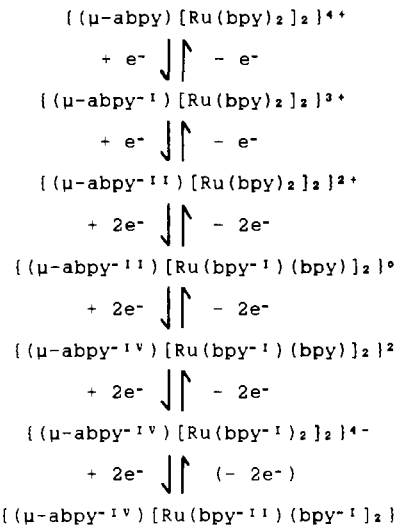

weak features at long wavelengths can be interpreted as intraligand (IL) bands from $abpy^{\bullet-}$ or $bpy^{\bullet-}$ which are enhanced in intensity because of perturbation by metal coordination[23a] or as interligand charge-transfer transitions (ILCT).[23b]

$Ru(abpy)_3]^m$. The ^1H NMR spectra (Figure 3) have allowed us to distinguish between the *fac* and *mer* isomers because of the quite different symmetries (C_3 and C_1, respectively). Infrared spectra show greater band intensities due to the higher polarity of the *fac* isomer in the region around 1400 cm^{-1}. The long-wavelength metal-to-ligand charge-transfer (MLCT) bands of both isomers differ in terms of a broader band for the less symmetrical *mer* isomer (Figure 4); such bands are really composed of several transitions of different intensities from three filled d orbitals of ruthenium(II).[24] The *mer* isomer also shows a more pronounced peak at about 286 nm (Figure 4).

The UV/vis-spectroelectrochemical data confirm the stepwise addition of electrons to the coordinated abpy ligands. Despite the equivalence of three ligands, there is an unusually[2,7h] large splitting of potentials which we attribute to a strong Coulombic interaction between the primarily electron-accepting azo groups with their considerably lengthened N–N bond on reduction. Additional evidence for this interpretation comes from the larger splitting of redox potentials (Table IV) for the *fac* isomer with its exclusively cis-arranged and thus closer situated azo coordination centers. The broad long-wavelength features in the highly reduced species can be tentatively assigned to interligand charge-transfer transitions (ILCT).[23b]

The EPR spectra of the both isomeric singly reduced forms $[Ru(abpy^-)(abpy)_2]^{\bullet+}$ show the expected[7h,10] broad lines, the lack of resolution from metal or ligand hyperfine coupling being due to electron hopping between equivalent sites.[10a-c] There is a decrease of line width at lower temperatures; however, the small g anisotropy precludes the determination of g components. The slightly lower g factors (Table V) than the free electron value of 2.0023 indicate the presence of low-lying excited states.[7h,20a]

$[Ru(abpy)_2(bpy)]^m$. Two diastereoisomers out of the three posible ones (**3**) could be isolated chromatographically, the third isomer being formed only in a small amount. Of the two isolated complexes, one is unsymmetrical (β form) whereas the other is obviously one of the α isomers with C_2 symmetry. While it was not possible to make comprehensive ^1H NMR assignments, we assume that the α_1 isomer is formed and not the α_2 species which would have the space-demanding "free" pyridyl groups in cis positions. Strong evidence for this assignment comes from the splitting between the first two abpy-centered reductions which is significantly larger for the β isomer with cis-positioned azo groups than for the isolated α isomer (α_1) with azo groups in trans positions (Table IV); the cis arrangement of azo functions (**3**)[25] in the α_2 conformation should result in a potential splitting $E_1 - E_2$ very similar to that for the β isomer.

Scheme III

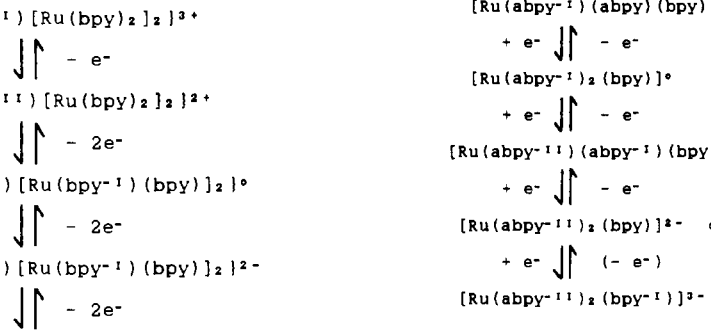

The UV/vis absorption spectra are less different here than in the case of the $Ru(abpy)_3$ complexes; two MLCT bands for transitions to the π^* orbitals of abpy and bpy are observed for the nonreduced (2+) species (Figure 5). The spectroelectrochemistry may be interpreted in terms of Scheme III, in which the two oxidation states $[Ru(abpy)_2(bpy)]^{-/2-}$ are of particular interest. The results in Table VI suggest that the $abpy^-$ ligand is more easily reduced than coordinated bpy^0.

EPR studies of the reduced complexes $[Ru(abpy^-)(abpy)(bpy)]^{\bullet+}$ yielded a surprising result. Only the β isomer gave a detectable EPR spectrum at ambient temperature; the signal of the α_1 isomer emerged only after freezing out at 180 K. As the line widths of both forms at low temperature confirm (Figure 6, Table V), the α_1 isomer exhibits a much broader signal than the β isomer or, for that matter, other related complexes such as the isomers of $[Ru(abpy^-)(abpy)_2]^{\bullet+}$. We attribute this peculiar dissimilarity to a very different activation energy for intramolecular ligand-to-ligand electron transfer (electron hopping)[7h,10a-c] since the α_1 isomer is distinguished from all other species by containing *exclusively* trans-positioned azo functions at octahedral ruthenium(II). Apparently, the strong asymmetry of the azo-2-pyridyl acceptor function has allowed us to observe the configurational dependence (cis vs trans) of interligand electron exchange. The effect of temperature suggests qualitatively that the barrier is significantly lower in the case of the α_1 isomer, with its lack of cis-positioned azo groups.

Summarizing, we have established the significance of configurational isomerism for intramolecular electron-exchange phenomena in the case of complexes with the very special 2,2′-azobis(pyridine) ligands. The free 2-pyridyl groups and azo nitrogen atoms e.g. of the complexes $[Ru(abpy)_3]^{2+}$ and $[Ru(abpy)_2(bpy)]^{2+}$ can be used to add further metal complex components such as $[Ru(bpy)_2]^{2+}$;[26] the synthesis and study of corresponding oligonuclear complexes is currently in progress.

Acknowledgment. This work was supported by a scientific exchange program between the Czech Academy of Sciences (ČSAV) and the Deutsche Forschungsgemeinschaft (DFG).

(23) (a) Braterman, P. S.; Song, J.-I.; Kohlmann, S.; Vogler, C.; Kaim, W. *J. Organomet. Chem.* **1991**, *411*, 207. (b) Heath, G. A.; Yellowlees, L. J.; Braterman, P. S. *J. Chem. Soc., Chem. Commun.* **1981**, 287; *Chem. Phys. Lett.* **1982**, *92*, 646.

(24) Belser, P.; Daul, C.; von Zelewsky, A. *Chem. Phys. Lett.* **1981**, *79*, 596.

(25) The α_2 conformation was established crystallographically for one isolated isomer of $[Ru(pap)_2Cl_2]$: Seal, A.; Ray, S. *Acta Crystallogr., Sect. C: Cryst. Struct. Commun.* **1984**, *C40*, 929.

(26) Matheis, W. Ph.D Thesis, University of Stuttgart, 1993.